Catchment Boundaries of Ocean Drainage Basins

Philip Craig

February 27, 2019

Contents

1 Introduction

This document describes the data and method used to construct the boundaries between the drainage basins of each ocean basin. These will be used primarily as the release points for trajectories in chapter 5 and also to evaluate moisture fluxes in chapter 4 of Craig (2018) - this documentation is also adapted from chapter 2 of Craig (2018). Figure 1 shows the drainage basins for the major oceans and seas. The aim is to use topographic datasets (section 4) to approximate the catchment boundaries and the ocean drainage basins they surround. These will not precisely match Figure 1 as they are approximated and also because different extents of the ocean drainage basins will be used to suit this study.

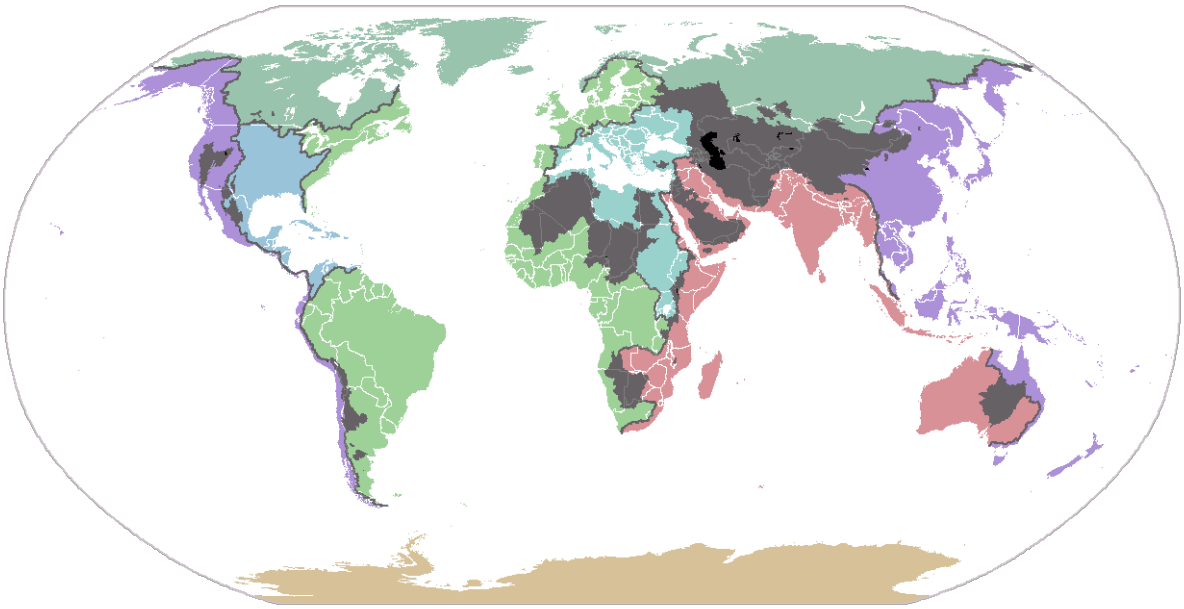

Figure 1: Depiction of the major ocean drainage basins from www.radicalcartography.net. Light green regions drain into the Atlantic Ocean, dark green into the Arctic Ocean, purple into the Pacific Ocean, red into the Indian Ocean, brown into the Southern Ocean, blue into the Caribbean Sea and turquoise into the Mediterranean Sea. Grey regions are endorheic basins which do not drain into the global ocean. The catchment boundaries in this map were identified using USGS Hydro1k data.

2 Terminology

Some key terminology which will be used throughout this documentation is defined here.

- **Drainage basin/catchment area**: area of land in which the precipitation gathers and flows towards a common outlet;
- **Catchment boundary**: a physical line which seperates drainage basins;
- **Continental divide**: a boundary between the drainage basins of different oceans.

3 Method

Using Figure 1 as a template, the various datasets delineating drainage basins (section 4) were overlain on a map of the ETOPO5 topography and segments of the boundaries were approximated by manually selecting points along the boundaries to create segments as a suitable dataset defining the catchment boundaries does not exist. To obtain points between the end points of the segments, linear interpolation was used to find points spaced approximately 75 km apart which is approximately within the resolution of the ECMWF model (Dee *et al.*, 2011). Some studies which present ocean drainage basins have used river-routing datasets (e.g. Rodriguez *et al.*, 2011; Wills and Schneider, 2015) and others have used maximum topography (Levang and Schmitt, 2015; Singh *et al.*, 2016). However, the accuracy available from this method is sufficient enough not to require a river-routing dataset as it is within the horizontal resolution of the ECMWF model (Dee *et al.*, 2011). Using maximum topograpy is also problematic as catchment boundaries do not neccessarily follow maximum topography. This problem can be seen in Singh *et al.* (2016) where the catchment boundaries leave the land and cross over seas and rivers.

4 Datasets

This section describes the datasets used to construct the ocean catchment boundaries.

4.1 HydroSHEDS

The Hydrological data and maps based on Shuttle Elevation Derivatives at multiple Scales (HydroSHEDS; Lehner *et al.*, 2008) dataset from the United States Geological Survey (USGS) uses high resolution satellite data from the Shuttle Radar Topography Mission (SRTM) to determine the boundaries of river catchment areas. Currently at version 1.2 (Lehner *et al.*, 2013), HydroSHEDS covers most of the globe at resolutions of 3 arc-seconds, 15 arc-seconds and 30 arc-seconds. HydroSHEDS is available from www.hydrosheds.org. Note that the previous version (1.1) was used in this work and is restricted between 60°N and 60°S (Figure 2) although this has been extended beyond these limits in version 1.2 (Lehner *et al.*, 2013). HydroSHEDS was used to define the American, African and South-East Asian catchment boundaries (Figure 6-8), as well as the Arctic catchment boundary along Eurasia (Figure 9) and the boundary of the River Plate drainage basin which forms part of the Southern Ocean catchment boundary (Figure 10).

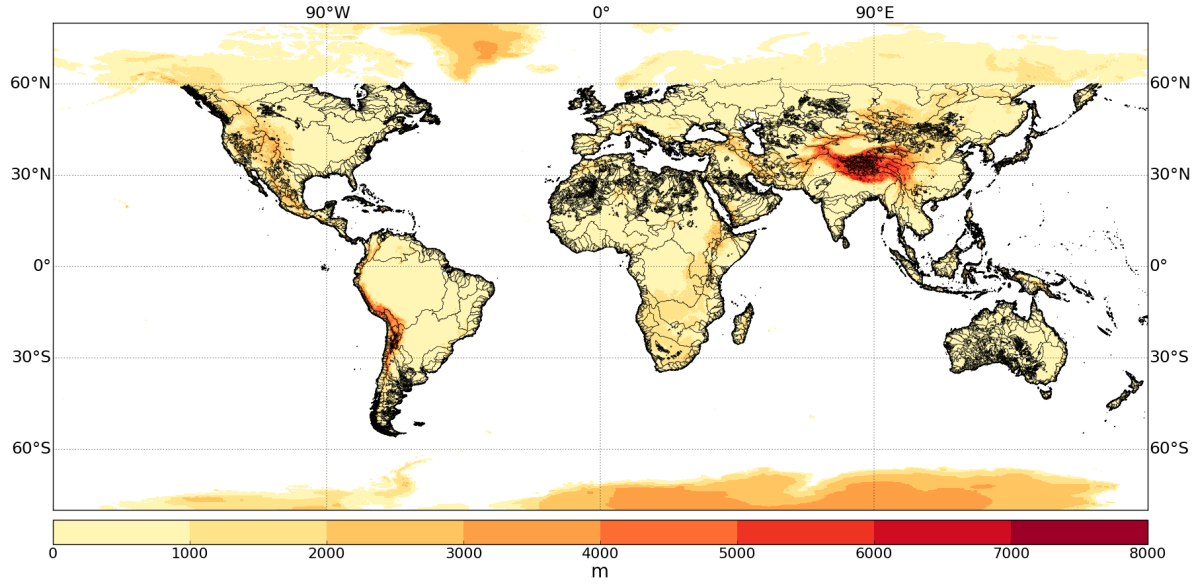

Figure 2: Continental topography from the ETOP05 dataset (contours) and river catchment boundaries from the HydroSHEDS dataset (Lehner *et al.*, 2008) (black lines).

4.2 ETOPO05

ETOPO5 is a global dataset of topography (contours, Figure 2) and bathymetry provided by the National Oceanic and Atmospheric Administration on a 5-minute latitude/longitude grid (National Geophysical Data Center, 1993) with 12 points per degree. When defining the catchment boundaries, the ETOP05 dataset shows which topographic features the catchment boundaries are located along and when no catchment boundary data were available (Scandinavia, western Russia, Alaska) the topography acted as a guide based on Figure 1.

4.3 Geofabric

The Australian Hydrological Geospatial Fabric (Geofabric) is a digital database constructed by the Bureau of Meteorology of surface and groundwater features which records the spatial relationships between important hydrological features. Input data for Geofabric includes a 9 second digital elevation model which is used to construct hydrology reporting regions (Bureau of Meteorology, 2015). The topographic drainage divisions of Geofabric are shown in Figure 3. Geofabric is used for the Australian parts of the South-East Asian and Southern Ocean catchment boundaries (Figures 8 and 10 respectively) instead of HyroSHEDS as it provides only the eleven major hydrological regions for Australia rather than every single river drainage basin in HydroSHEDS (Figure 2). The data is available from the Geofabric webpage: http://www.bom.gov.au/water/geofabric/.

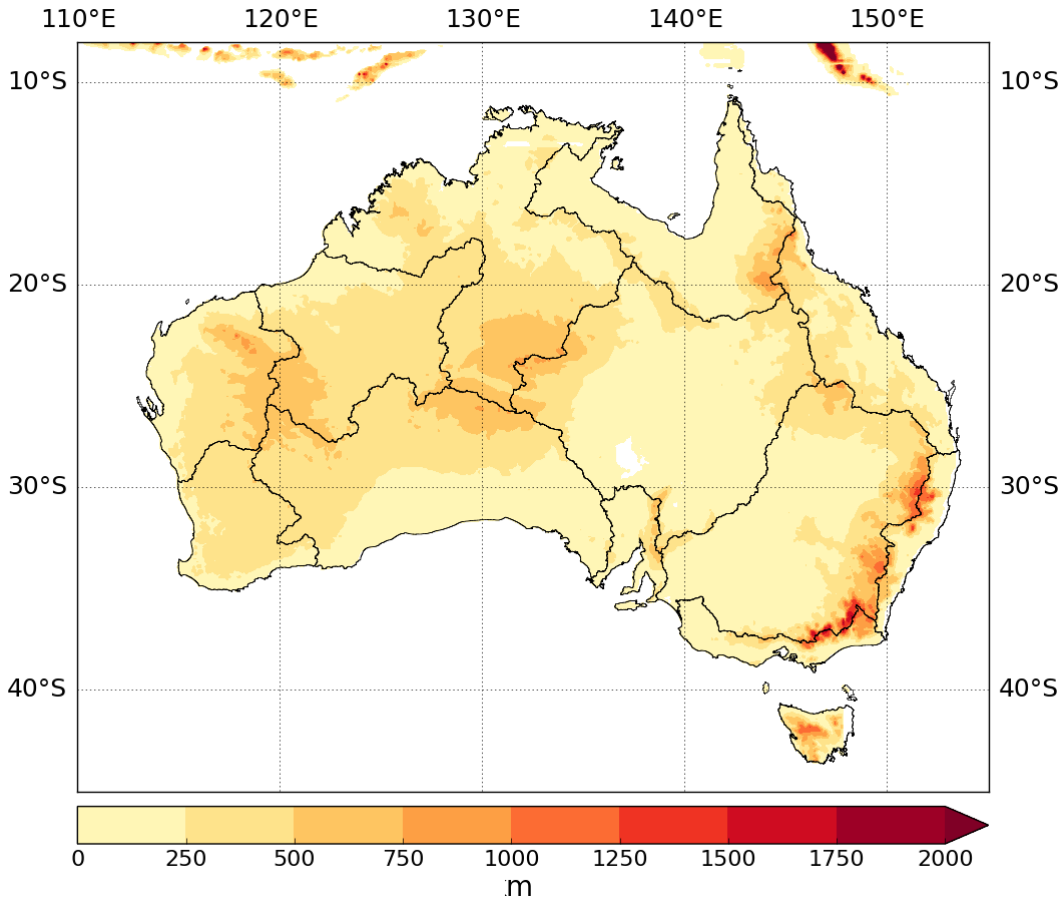

Figure 3: The catchment boundaries for Australia's major drainage basins (Bureau of Meteorology, 2015) (black lines) overlain on topography from the ETOP05 dataset (contours).

4.4 Natural Resources Canada

Figure 4 shows the Canadian boundaries of the drainage basins for the Atlantic Ocean, Arctic Ocean, Hudson Bay and Pacific Ocean. This data is part of the Atlas of Canada and was obtained from Natural Resources Canada. The ocean drainage basin dataset (Natural Resources Canada, 2009) was developed from the hydrographic layers of a global digital dataset produced by the United States National Imagery and Mapping Agency (NIMA). Similar to Geofabric, Figure 4 provides only the major hydrological regions for Canada and also extends further north than version 1.1 of HydroSHEDS (Figure 2). This dataset is used to define the Canadian part of the Arctic catchment boundary (Figure 9).

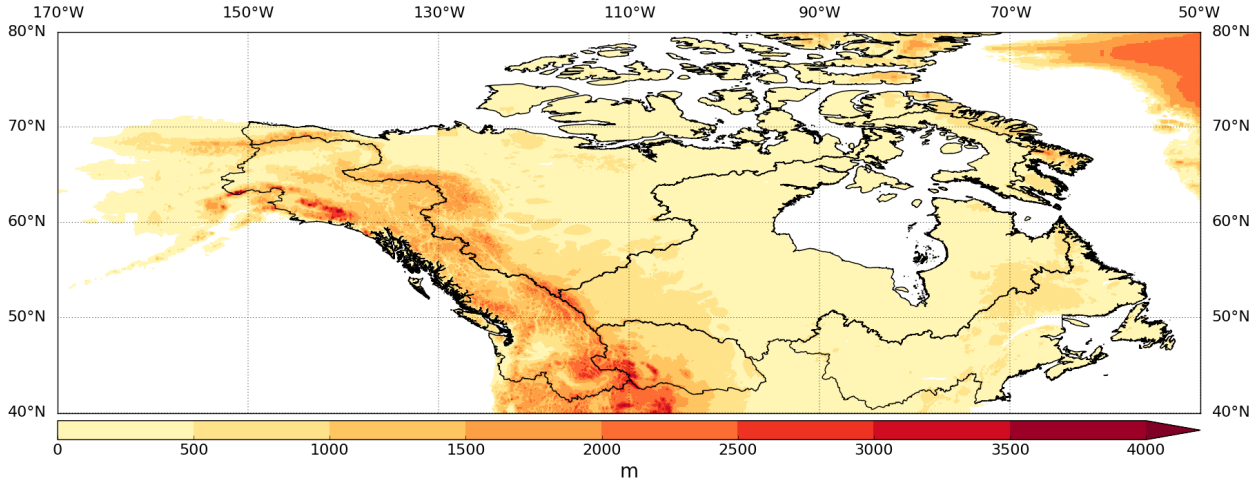

Figure 4: Canadian drainage basins from Natural Resources Canada (black lines) overlain on ETOT05 topography (contours).

4.5 Ice Sheet Mass Balance Inter-Comparison Exercise (IMBIE)

Figure 5 shows the drainage basins of Greenland from the ice sheet mass balance inter-comparison exercise (IMBIE). The drainage divides in Figure 5 are actually ice motion divides (Rignot and Mouginot, 2012) which are based on changes in direction of ice flow. Rignot and Mouginot (2012) estimated these divides using various satellite data: Envisat Advanced Synthetic-Aperture Radar (ASAR), Advanced Land Observation System (ALOS)'s Phase-Array L-band SAR (PALSAR) and the RADARSAT-1 SAR. The data for the Rignot and Mouginot (2012) divides are available at http://imbie.org/ and used to define the Arctic catchment boundary across Greenland (Figure 9).

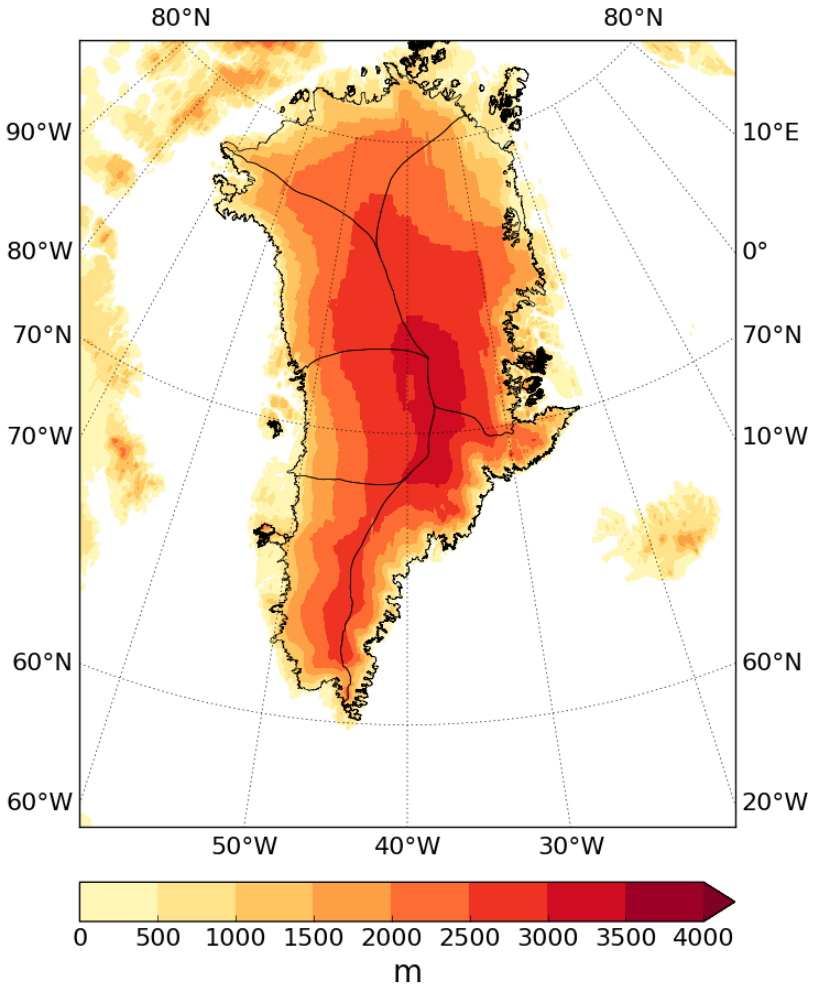

Figure 5: Rignot and Mouginot (2012) Greenland ice sheet boundaries (black lines) overlain on ETOP05 topography (contours).

5 Catchment boundaries

Each catchment boundary is described below. Overall there are nine catchment boundaries as the boundaries surrounding the Arctic and Southern Ocean drainage basins are split into three sectors (Atlantic, Indian and Pacific). Table 1 shows the longitude-latitude co-ordinates of the start and end points as well as the number of points of each boundary. The catchment boundaries are shown individually in Figures 6-10 and all together in Figure 11.

Table 1: Number of points in each catchment boundary and the longitude-latitude co-ordinates of the start and end points of each boundary. The Arctic and Southern Ocean catchment boundaries are split into three sectors based on which of the other three oceans it seperates the Arctic or Southern Ocean from.

catchment boundary	number of points	start	end
Americas	155	(117.45°W, 52.03°N)	(71.03°W, 15.32°S)
Africa and Middle East	214	(41.98°E, 40.08°N)	(20.22°E, 35.00°S)
South-East Asia	165	(92.18°E, 32.71°N)	(144.97°E, 20.48°S)
Arctic Atlantic	197	(117.45°W, 52.03°N)	(41.98°E, 40.08°N)
Arctic Indian	103	(41.98°E, 40.08°N)	(92.18°E, 32.71°N)
Arctic Pacific	220	(92.18°E, 31.71°N)	(117.45°W, 52.03°N)
Southern Atlantic	185	(71.03°W, 15.32°S)	(20.22°E, 35.00°S)
Southern Indian	184	(20.22°E, 35.00°S)	(144.97°E, 20.48°S)
Southern Pacific	212	(144.97°E, 20.48°S)	(71.03°W, 15.31°S)

5.1 Americas

The continental divide between the Atlantic and Pacific drainage basins follows the spine of the Rocky Mountains (Figure 6) starting at the Snow Dome at 52°N in Canada. The Snow Dome is a "triple divide" or "hydrological apex" *i.e.* a point where three drainage basins meet. Although the Snow Dome is taken as the hydrological apex of the Atlantic, Arctic and Pacific drainage basins in this study, Triple Divide Peak further South in Montana can also be considered to be the hydrological apex of North America depending on whether Hudson Bay is included in the Atlantic or Arctic basin. Here, Hudson Bay is included in the Atlantic basin.

After the southern end of the Rocky Mountains the boundary follows the mountain ranges in Mexico and Central America, almost following the coastline in Central America. The boundary joins the Andes in Colombia - a section which was troublesome for Levang and Schmitt (2015) and Singh *et al.* (2016) as their use of maximum topography caused the eastern branch to be included in their boundary but the rivers between the eastern and western branches drain into the Atlantic basin. The boundary follows the spine of the Andes until 15°S near the border between Peru and Bolivia.

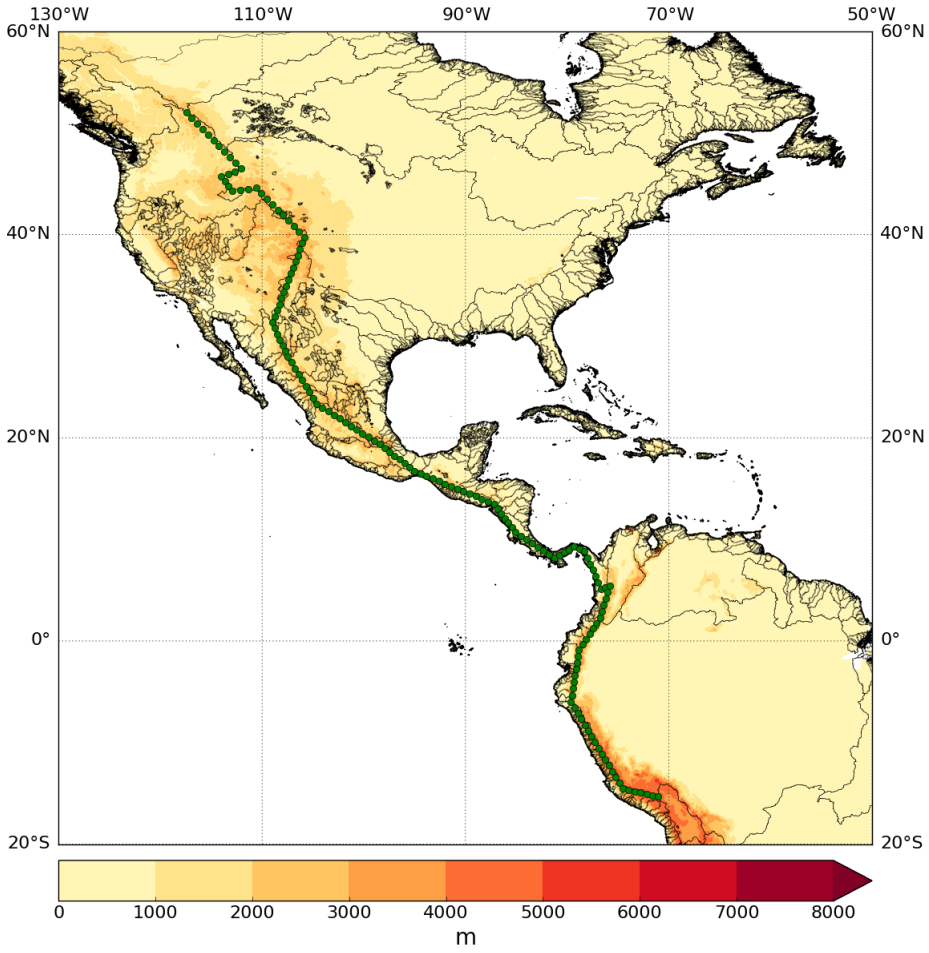

Figure 6: Points used for the American catchment boundary (green circles) overlain on HydroSHEDS data (black lines) and ETOP05 topography (contours).

5.2 Africa and the Middle-East

This catchment boundary serparates the drainage basins of the Atlantic and Indian Oceans with the Mediterranean Sea included in the Atlantic drainage basin. The boundary shown in Figure 7 is the combination of the boundaries from Figure 1 that the Indian Ocean basin has with the Atlantic and Mediterranean basins. The boundary between the Atlantic and Indian Ocean drainage basins begins in the mountains of north-west Turkey, follows the mountains in Syria, Lebanon and Israel into the Sinai Peninsula and follows the mountains along the Egyptian Coast before cutting through Ethiopia to Lake Victoria. South of Lake Victoria, the boundary cuts through Tanzania and follows the northern edge of the River Zambezi drainage basin westwards and the western edge of the Okavango basin before cutting south-east along the northern edge of the Orange basin and following the southern edge round to Cape Agulhas.

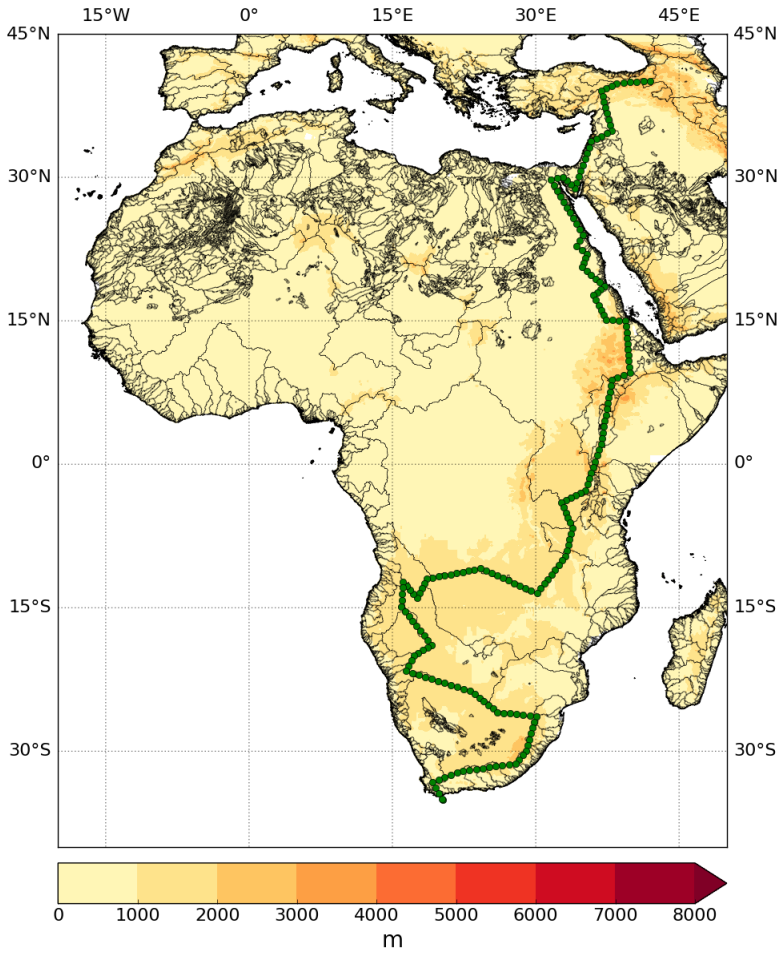

Figure 7: Points used for the African and Middle-Eastern catchment boundary (green circles) overlain on HydroSHEDS data (black lines) and ETOP05 topography (contours).

Figure 7 represents an improvement compared to Singh *et al.* (2016) where there are several errors in the location of the catchment boundary. In the north it follows the Zagros mountains before cutting acrosss the Red Sea into the middle of the Sahara Desert, then crossing the Red Sea again before following the maximum topography along a path more similar to Figure 7. The Singh *et al.* (2016) catchment boundary errneously suggests that the Tigris and Euphrates rivers drain into the Mediterranean Sea and also cuts across the River Nile and Red Sea in an unphysical manner. The catchment boundary in Figure 7 is much more realistic and the HydroSHEDS data clearly shows the large catchment area for the Nile which extends south of the equator to Lake Victoria.

5.3 South-East Asia

The boundary between the drainage basins of the Indian and Pacific Oceans is depicted in Figure 8. Starting at 32°N on the Tibetan Plateau, the boundary extends southwards through Burma, Thailand and Malaysia. It is after leaving Malaysia that the boundary shown in Figure 8 differs from that shown in Figure 1. In Figure 1, the boundary cuts straight through the Java and Banda Seas then rejoins the land on Australia east of Darwin. In Figure 8 however, the boundary moves onto the west coast of Sumatra which it follows until Java and then cuts straight across to New Guinea and southwards across the Torres Strait before terminating in Queensland at 20°S. The approach used here also differs from the boundaries shown by Wills and Schneider (2015) and Levang and Schmitt (2015). The former also follow the west coast of Sumatra and Java but enter Australia at a similar location to Figure 1, while the latter use maximum topography and the boundary cuts across the islands further to the north (Borneo and Sulawesi) and continues further south into Australia, terminating at 30°S. Placing the catchment boundary along 8°S (Figure 8) avoids the region of strong moisture flux convergence (Craig, 2018) and means that there is consistency between the western/eastern boundaries of the Pacific/Indian Oceans used in Craig *et al.* (2017) and chapters 4/5 of Craig (2018).

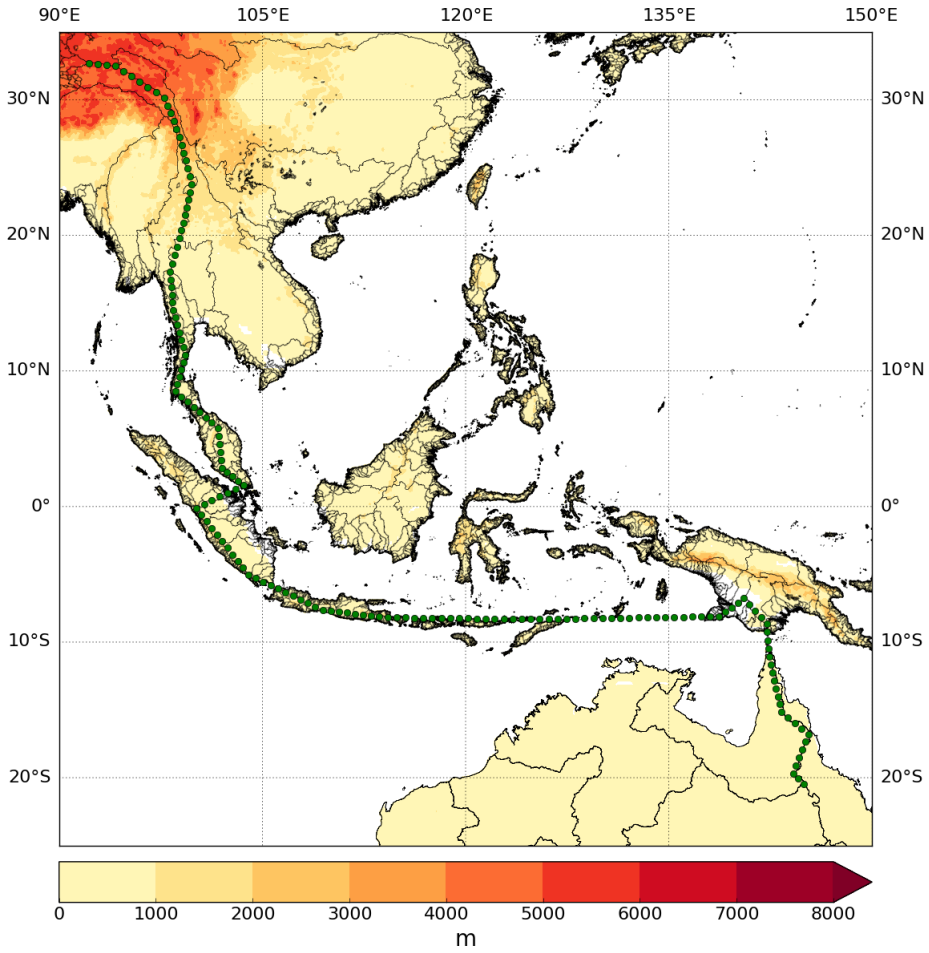

Figure 8: Points used for the South-East Asian catchment boundary (green circles) with HydroSHEDS and Geofabric data (black lines) and ETOP05 topography (contours).

5.4 The Arctic

The boundary for the Arctic Ocean drainage basin is shown in Figure 9. There are several key differences between the Arctic boundaries shown in Figures 9 and 1. Firstly, the Atlantic sector of the boundary in Figure 9 starts at the Snow Dome (red circle on North America, Figure 9) instead of Triple Divide Peak (see section 5.1 and blue triangle in Figure 9) and therefore Hudson Bay is not included in the Arctic drainage basin for this estimate. The drainage divide crosses Greenland following the ice sheet drainage boundaries from Rignot and Mouginot (2012) then extends eastwards to Svalbard and turns southwards to Scandinavia. This shape of the boundary includes the Nordic and Labrador Seas in the Atlantic Ocean, where deep convection occurs.

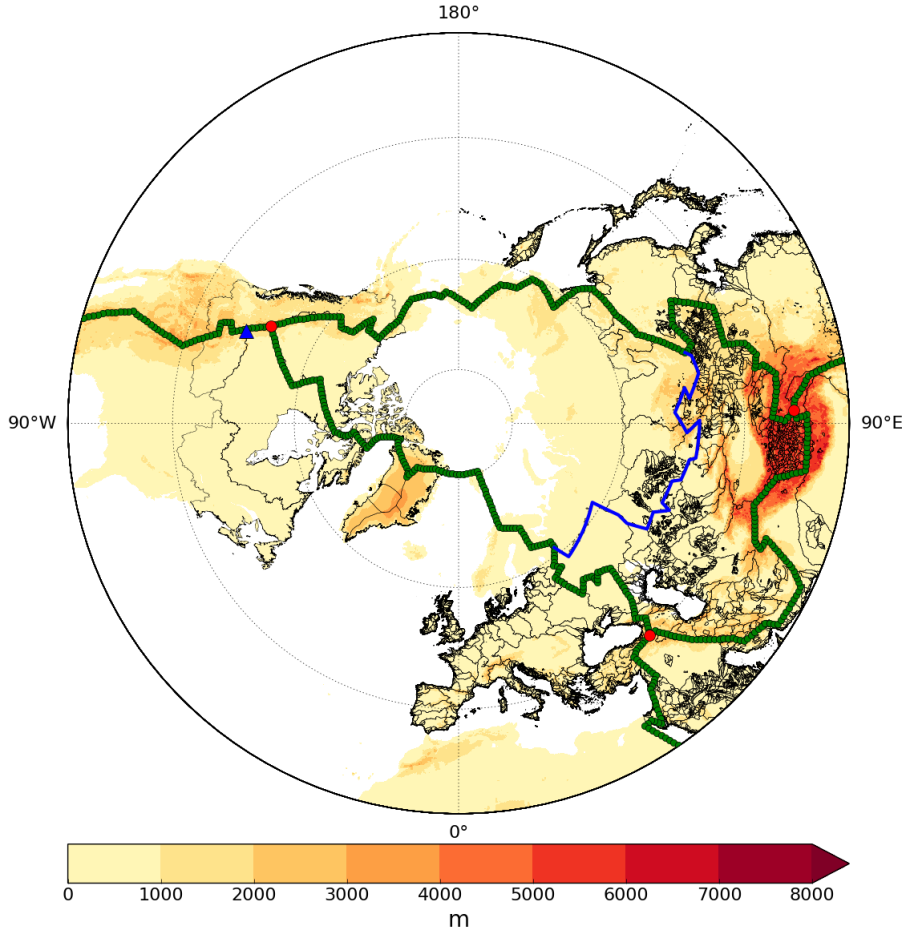

Figure 9: Points used for the catchment boundary of the Arctic Ocean drainage basin (green circles) overlain on the catchment boundaries from Natural Resources Canada, Rignot and Mouginot (2012) and the HydroSHEDS dataset and ETOP05 topography. The large red circles indicate the intersections of the Arctic catchment boundary with the American, African and South-East Asian catchment boundaries. The blue triangle indicates the location of Triple Divide Peak on the American catchment boundary and the blue line across northern Eurasia shows the northern boundary of the Central Asian endorheic basin.

A key feature of the Arctic boundary shown in Figure 9 is the southerly extent through Iran and along the Himalayas rather than tracking further north through Russia, Kazakhstan and Mongolia. The purpose of this is to the include the large Central Asian endorheic basin in the Arctic drainage basin. For such regions $E - P \approx 0$ (Stohl and James, 2005) and there is no relationship between the moisture budgets of these regions and SSS so would be unneccessary to consider this basin separately. Including the Central Asian endorheic basin in the Arctic drainage basin means that the Atlantic sector of the Arctic boundary terminates in northern Turkey and the boundary between the Arctic and Indian Ocean catchment areas extends from northern Turkey to the eastern Tibetan

Plateau.

The Pacific sector of the Arctic boundary cuts north-east across China, through Russia and across the Bering Strait at 65°N (the northern limit of the Pacific Ocean). Before completing the boundary and returning to the Snow Dome in Canada, it shifts to the north-east after the Bering Strait to include the drainage basin of the River Yukon which flows into the Bering Sea (part of the Pacific Ocean). Levang and Schmitt (2015) failed to use the correct path of the boundary through Alaska by using maximum topography. Instead, their boundary cuts straight through the middle of Alaska, straight through the Yukon basin which almost reaches the north coast. The boundaries in Figures 1 and 9 show the correct route of the continental divide.

5.5 Southern Ocean

The boundary of the Southern Ocean was somewhat simpler to construct (Figure 10). A northern extent of the Southern Ocean of 35°S was chosen as this matches the approximate southern limits of Africa and South-West Australia. There are four land areas which drain into the Southern Ocean: Antarctica, Australia, New Zealand and South America. Antarctica is obviously in the centre of the Southern Ocean and the region of the north island of New Zealand which is north of 35°S is too small to contribute any significant amount of runoff to the moisture budget. Australia, however, has rivers which drain into the Southern Ocean, as shown by Figure 3, which are included in the Southern Ocean drainage basin (Figure 10). In South America the mouth of the River Plate enters the ocean between 35°S and 36°S. The location of this outflow presents a problem as it feeds water into the region of the confluence between the northwards Falklands current and the southwards Brazil current. The surface currents then travel eastwards as part of the subtropical gyre and are then recirculated northwards. It could therefore be equally valid to include the River Plate basin in either the Atlantic or Southern Ocean drainage basin as the discharge from the River Plate likely contributes to the water budget of both oceans. However, any attempt to determine the destination of River Plate outflow and which ocean's water budget is has most effect on would overcomplicate the matter further so the River Plate basin was simply included in the Southern Ocean drainage basin where it initially enters anyway.

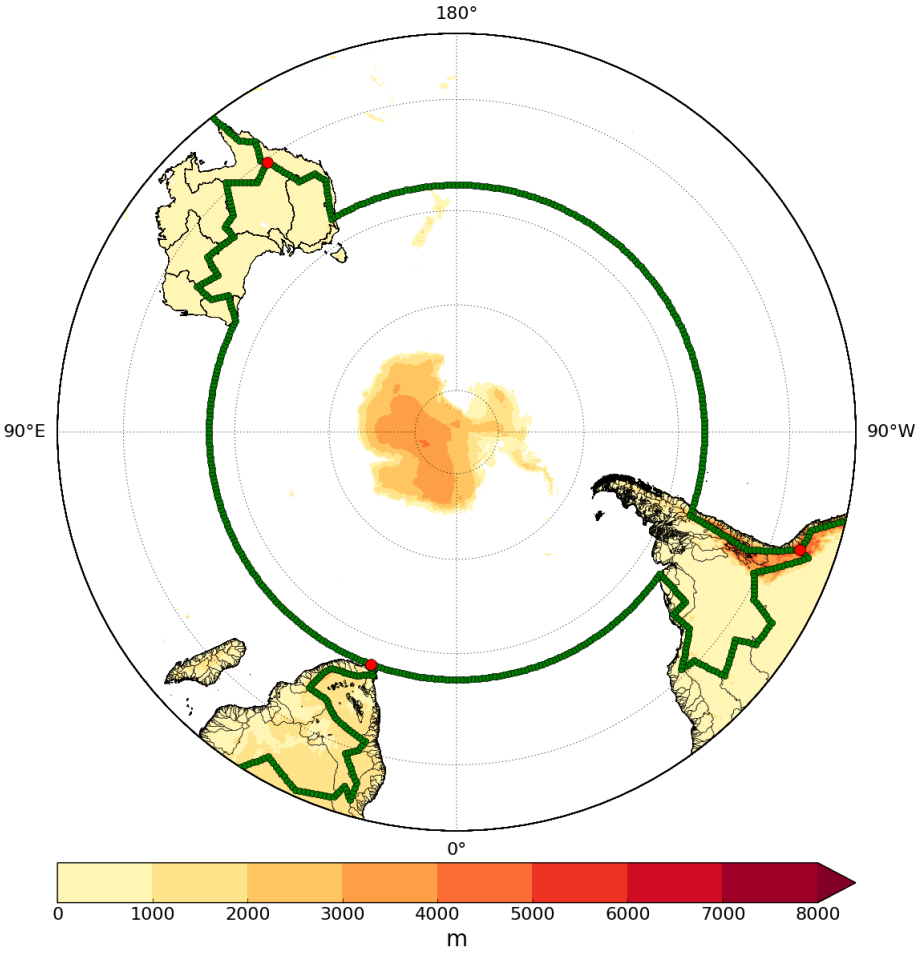

Figure 10: Points used for the catchment boundary of the Southern Ocean drainage basin (green circles) overlain on Geofabric catchment boundaries (Figure 3) HydroSHEDS data and ETOP05 topography. The large red circles indicate the intersections of the Southern Ocean catchment boundary with the American, African and South-East Asian catchment boundaries.

6 The Ocean Drainage Basins

The catchment boundaries described in sections 5.1-5.5 are shown in Figure 11. Together they form the boundaries of the drainage basins for the Atlantic, Pacific, Indian, Arctic and Southern Oceans. From Figure 11 it is clear that despite the greater size of the Pacific Ocean the area of land included in the Atlantic drainage basin is much larger than that for the Pacific drainage basin. Most of the North and South American continents drain into the Atlantic Ocean, as do most of Africa and Greenland and all of Europe. Only narrow strips near the western coasts of the Americas drain into the Pacific Ocean, along with part of eastern Asia, the Maritime Continent and a tiny strip of eastern Australia. The Indian Ocean drainage basin includes the Arabian Peninsula and Indian subcontinent, plus a mostly narrow strip of eastern Africa and much of the northern and western regions of Australia. Most of Russia drains into the Arctic Ocean along with some of Alaska and northern Canada and Greenland. Antarctica is the main land region in the Southern Ocean drainage basin, the other land regions in this drainage basin are New Zealand, much of southern and eastern Australia, and the River Plate basin in South America plus all the land south of 35°S.

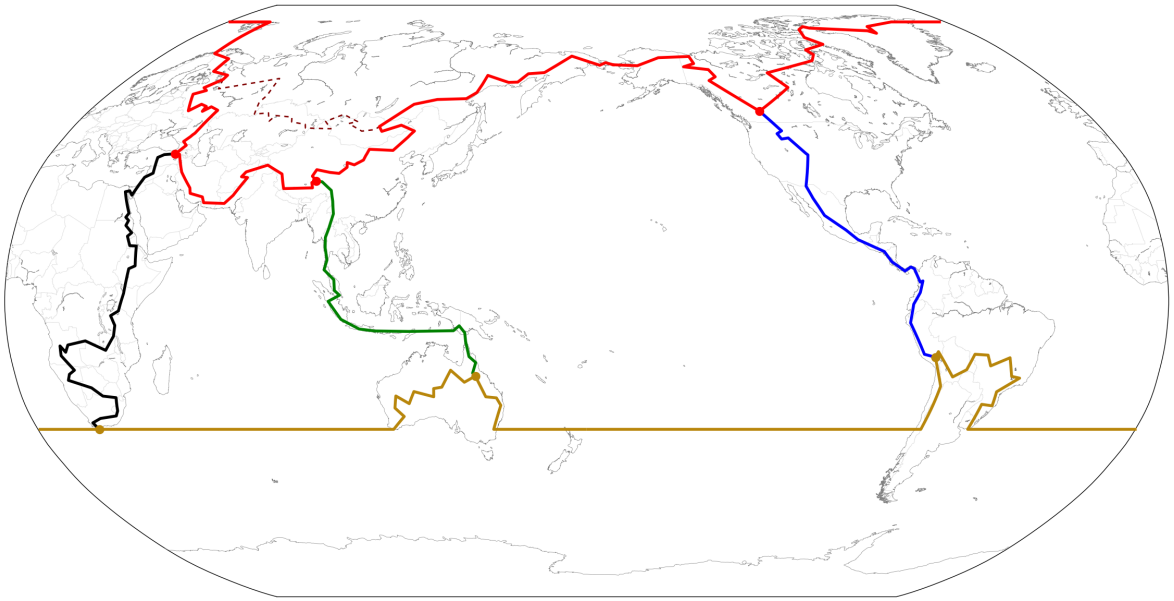

Figure 11: All the catchment boundaries: Americas (blue), Africa and Middle East (black), South-East Asia (green), Arctic (red) and Southern (gold). The red/gold dots indicate the end points of the different sectors of the Arctic/Southern catchment boundaries. The dashed maroon line is the northern boundary of the Central Asian endorheic basin.

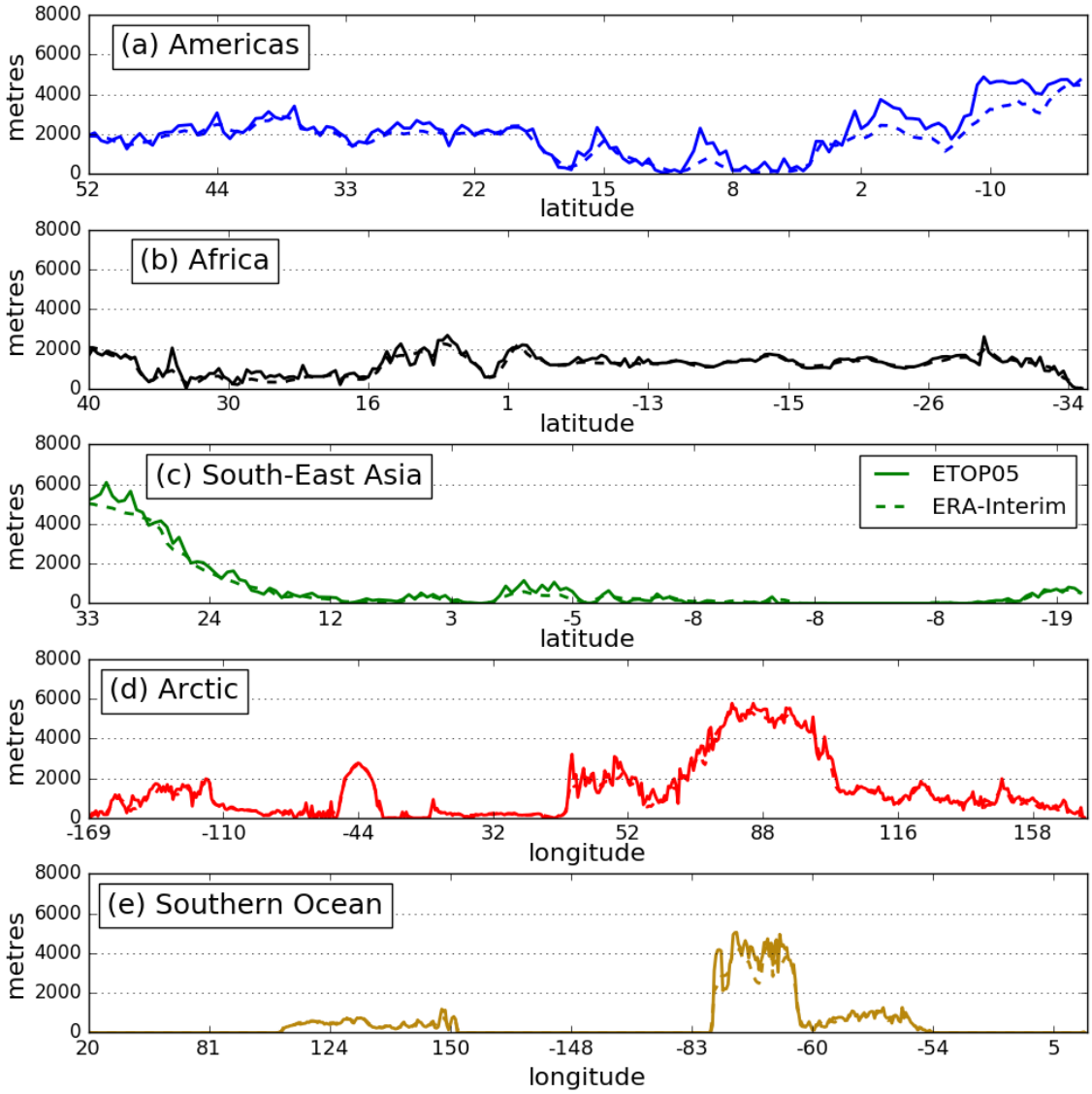

Figure 12: Comparison between orography from ETOP05 (solid lines) and ERA-Interim (dashed lines) along each catchment boundary. Note that ERA-Interim does not provide an estimate of orography from the IFS but it can be calculated using the geopotential (Φ) where the orography is Φ/g. The estimates are plotted against distance along the catchment boundaries but labelled by either latitude or longitude.

Figure 12 shows that the orography along the catchment boundaries shown in Figure 11 is generally well estimated by ERA-Interim compared to the higher resolution ETOP05 dataset. The ERA-Interim orography (Φ/g, where Φ is the geopotential) performs worst along the Andes in South America along the American and Southern Ocean catchment boundaries (Figure 12(a,e)). As the Andes is quite a narrow mountain range (Figure 6) the underestimation of the height of the orography is likely due to the lower resolution of the ECMWF model. However, the shape of the orography along the catchment boundaries is generally captured by ERA-Interim and the underestimation of the height of the orography is not substantial.

References

Bureau of Meteorology (2015). *Australian Hydrological Geospatial Fabric (Geofabric) Product Guide*. Canberra. version 3.0.

Craig, P.M. (2018). *The Atlantic/Pacific Atmospheric Moisture Budget Asymmetry: The Role of Atmospheric Moisture Transport*. Ph.D. thesis, University of Reading.

Craig, P.M., Ferreira, D., and Methven, J. (2017). The contrast between Atlantic and Pacific surface water fluxes. *Tellus A*, **69**(1330454).

Dee, D.P., Uppala, S.M., Simmons, A.J., Berrisford, P., Poli, P., Kobayashi, S., Andrae, U., Balmaseda, M.A., Balsamo, G., Bauer, P., Bechtold, P., Beljaars, A.C.M., van de Berg, L., Bidlot, J., Bormann, N., Delsol, C., Dragani, R., Fuentes, M., Geer, A.J., Haimberger, L., Healy, S.B., Hersbach, H., Holm, E.V., Isaksen, L., Kållberg, P., Köhler, M., Matricardi, M., McNally, A.P., Monge-Sanz, B.M., Morcrette, J.-J., Park, B-.K., Peuby, C., de Rosnay, P., Tavolato, C., Thépaut, J.-N., and Vitart, F. (2011). The ERA-Interim Reanalysis: configuration and performance of the data assimilation system. *Quarterly Journal of the Royal Meteorological Society*, **137**, 553–597.

Lehner, B., Verdin, K., and Jarvis, A. (2008). New global hydrology derived from spaceborne elevation data. *Eos, Transactions*, **89**, 93–94.

Lehner, B., Verdin, K., and Jarvis, A. (2013). HydroSHEDS Technical Documentation. Technical Report 1.2, US Geological Survey and World Wildlife Fund.

Levang, S.L. and Schmitt, R.W. (2015). Centennial Changes of the Global Water Cycle in CMIP5 Models. *Journal of Climate*, **28**, 6489–6502.

National Geophysical Data Center (1993). *5-minute Gridded Global Relief Data (ETOPO5)*. National Geophysical Data Center, NOAA. doi:10.7289/V5D798BF [accessed 10/02/2015].

Natural Resources Canada (2009). Atlas of Canada 1,000,000 National Frameworks Data, Hydrology. Government of Canada; Natural Resources Canada; Earth Sciences Sector; Canada Centre for Mapping and Earth Observation.

Rignot, E. and Mouginot, J. (2012). Ice flow in Greenland for the International Polar Year 2008-2009. *Geophysical Research Letters*, **39**(L11501).

Rodriguez, J.M., Johns, T.C., Thorpe, R.B., and Wiltshire, A. (2011). Using moisture conservation to evaluate oceanic surface freshwater fluxes in climate models. *Climate Dynamics*, **37**, 205–219.

Singh, H.K.A., Donohoe, A., Bitz, C.M., Nusbaumer, J., and Noone, D.C. (2016). Greater Moisture Transport Distances with Warming Amplify Interbasin Salinity Contrasts. *Geophysical Research Letters*, **43**, 8677–8684.

Stohl, A. and James, P. (2005). A Lagrangian Analysis of the Atmospheric Branch of the Global Water Cycle. Part II: Moisture Transports between Earth's Ocean Basins and River Catchments. *Journal of Hydrometeorology*, **6**, 961–984.

Wills, R.C. and Schneider, T. (2015). Stationary eddies and the zonal asymmetry of net precipitation and ocean freshwater forcing. *Journal of Climate*, **28**, 5115–5133.